Organic Electronics 13 (2012) 667–672

Contents lists available at SciVerse ScienceDirect

Organic Electronics

journal homepage: www.elsevier.com/locate/orgel

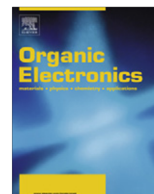

Modeling of charge transport across disordered organic heterojunctions

J. Cottaar [a,*], R. Coehoorn [a,b], P.A. Bobbert [a]

[a] Department of Applied Physics, Eindhoven University of Technology, P.O. Box 513, 5600 MB Eindhoven, The Netherlands
[b] Philips Research Laboratories, High Tech Campus 4, 5656 AE Eindhoven, The Netherlands

ARTICLE INFO

Article history:
Received 1 December 2011
Received in revised form 6 January 2012
Accepted 13 January 2012
Available online 1 February 2012

Keywords:
Organic semiconductor
Heterojunction
Charge transport
Disorder
Drift–diffusion equation
Monte Carlo

ABSTRACT

Organic electronic devices often consist of a sandwich structure containing several layers of disordered organic semiconductors. In the modeling of such devices it is essential that the charge transport across the organic heterojunctions is properly described. The presence of energetic disorder and of strong gradients in both the charge density and the electric field at the heterojunction complicates the use of continuum drift–diffusion approaches to calculate the electrical current, because of the discrete positions of the sites involved in the hopping transport of charges. We use the results of three-dimensional Monte Carlo simulations to construct boundary conditions in a one-dimensional continuum drift–diffusion approach that accurately describe the charge transport across the junction. The important effects of both short- and long-range Coulomb interactions at the junction are fully accounted for. The developed approach is expected to have a general validity.

© 2012 Elsevier B.V. All rights reserved.

1. Introduction

Devices based on thin organic films such as organic light-emitting diodes (OLEDs) are gaining in importance within the optoelectronics industry [1,2]. Typically, these devices consist of one or more layers of organic semiconductors sandwiched between two metal electrodes. OLEDs consisting of two layers were introduced by Tang et al. [3,4]. State-of-the-art OLEDs consist of more than two layers, including emission layers and hole and electron transport and injection layers [5,6]. In such devices a proper understanding of the charge transport across the interface between two organic semiconductors is crucial for accurate modeling of the optoelectronic characteristics. A key aspect is the energetic disorder present in organic semiconductors, which has a profound influence on the charge transport.

Charge transport in disordered organic semiconductors takes place through hopping of charge carriers between states localized on molecules or polymer segments. This gives rise to diffusion and, in the presence of an electric field, drift of charge carriers. Modeling of the current in an organic device can then be done following a one-dimensional drift–diffusion (1D-DD) approach, with a mobility μ and a diffusion coefficient D which is obtained from μ by using the generalized Einstein relation [7]. The dependence of μ on temperature, T, carrier density, n, and electric field, F, may be obtained from three-dimensional (3D) studies of hopping on a lattice of sites with a Gaussian energy disorder, performed by solving a master equation (ME) for the occupational probabilities of the sites [8]. For single-carrier single-layer devices, the accuracy of the 1D-DD approach was demonstrated by the very good agreement with full 3D-ME results for such devices [9]. Recently, the results of the 1D-DD approach were compared to those of 3D Monte Carlo (MC) simulations of such devices in which Coulomb interactions were fully included, with similarly encouraging results for carrier concentrations up to 1% [10]. The importance of the 1D-DD approach for the industrial development of organic devices lies in the ease and computational efficiency with which this approach can be applied in device modeling and parameter extraction [11].

It is also possible to model devices using the 1D master Eq. (1D-ME) approach introduced by Coehoorn and Van

* Corresponding author. Tel.: +31 40 2475638.
E-mail address: j.cottaar@tue.nl (J. Cottaar).

1566-1199/$ - see front matter © 2012 Elsevier B.V. All rights reserved.
doi:10.1016/j.orgel.2012.01.013

Mensfoort [12]. In this approach the charges are localized on a 1D chain of sites; hence, unlike the 1D-DD approach, this is a non-continuum approach. Since the 1D-ME approach considers charge hopping explicitly, it treats interfaces in a natural way and has been successfully applied to modeling experimental *J–V* characteristics of multi-layer devices [13]. In the present paper we will separate the treatment of interfaces from that of the bulk; since the non-continuum 1D-ME and continuum 1D-DD approaches yield similar results for the bulk [12], the choice of either method does not significantly change the results. We will mainly compare with the continuum 1D-DD method because of its widespread use.

For a multilayer device, the 1D-DD approach requires the use of an appropriate boundary condition at the interface between the different organic layers. We consider here only the case of an energy barrier, but other effects at the interface, such as different mobilities, can be treated similarly. Staudigel et al. obtained a boundary condition by considering the forward and backward hopping rates over the interface in conjunction with a reduction of the energy barrier by the local electric field [14]. Arkhipov et al. considered in addition the probability that a carrier that has hopped over the interface "escapes" further into the organic layer behind the interface [15]. Several modifications and applications of these semi-analytical approaches have been proposed [16–19]. Houili et al. were the first to perform 3D-MC simulations of charge transport across an organic heterojunction, including Coulomb interactions between the charges, and made a qualitative comparison with the semi-analytical approaches [20]. However, a systematic way to improve the 1D-DD approach using the results of 3D-MC simulations is still lacking.

The goal of this paper is to use the results of 3D-MC simulations to obtain general rules for improving the description of the charge transport across organic heterojunctions by the 1D-DD approach. In order to reach that goal we will apply both 3D-MC and 1D-DD modeling to a typical single-carrier bilayer device. In the next section we specify the structure of this device and discuss the 3D-MC modeling. In Section 3 we discuss the 1D-DD approach and start by proposing a simple boundary condition at the organic heterojunction. By a comparison with the 3D-MC modeling we then improve the 1D-DD approach in a step-by-step way. We introduce three improvements, including the introduction of a new boundary condition. We will show that when these improvements are used together, the 1D-DD approach can quantitatively reproduce the 3D-MC results. We also consider interface roughness and show that this has only a minor influence on the results. Section 4 contains a summary and conclusions.

2. Monte Carlo modeling of a single-carrier bilayer device

We model the organic semiconductors in our device as a cubic lattice of sites with a site density N_t and an intersite distance $a = N_t^{-1/3}$. Without loss of generality, we will consider hole transport in this work. The hole energy E_i of each site is fixed and taken at random from a Gaussian distribution with width (standard deviation) σ. We assume that there are no correlations in the hole energies, an assumption that has been found to lead to an accurate description of the current–voltage characteristics of hole-only devices based on poly (*p*-penylene vinylene) and polyfluorene [8]. Holes can hop from some site *i* to an unoccupied neighboring site *j* with a Miller–Abrahams [21] or Marcus [22] hopping rate. It has been shown that there is no important difference in the charge transport across interfaces for these two hopping rates [23], so we consider here only the simpler Miller–Abrahams rate:

$$W_{ij} = W_0 \exp(-[\Delta E + |\Delta E|]/2k_B T), \quad (1)$$

where W_0 is a material-dependent prefactor and $k_B T$ is the thermal energy. The energy change ΔE involved in the hop contains two contributions: (i) the difference in hole energies between sites *j* and *i* due to the disorder, and (ii) the potential difference between these sites. The latter contribution is due to the voltage applied over the device and the electrostatic interaction with other holes as well as with image charges in the electrodes.

The considered device structure and the involved energy levels (neglecting the effect of the space charge) are sketched in Fig. 1. At the left and right side of the bilayer, two additional layers of sites represent the identically chosen electrodes. Hops to and from the electrode are also assumed to take place with the rate given by Eq. (1). Apart from an energy barrier Δ between the tops of each Gaussian density of states (DOS) we take the two organic materials to be identical, using typical parameters: $\sigma = 0.09$ eV, $W_0 = 10^5$ s^{-1} and $N_t = 2 \times 10^{26}$ m^{-3} (corresponding to $a \approx 1.7$ nm). At room temperature (295 K), the mobility in the limit of zero carrier density and zero field is then 1.6×10^{-14} m^2/V s. The relative dielectric permittivity ϵ_r is taken to be 3. The total thickness of the device is $L = 12a \approx 20.4$ nm. This rather small thickness ensures that the interface plays a large role in determining the current density–voltage (*J–V*) characteristics. The organic–organic interface is located between the fifth and

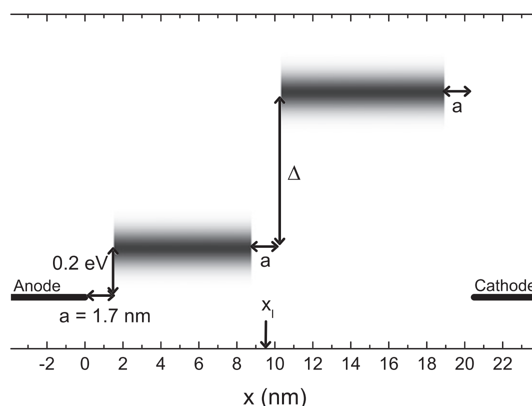

Fig. 1. Energy diagram for the device to which we apply our modeling, with a barrier Δ between the tops of the Gaussian hole densities of states – indicated by the shading – of the two disordered organic semiconductors. The energies shown are hole energies. The position x_I of the interface is indicated.

the sixth layers of organic sites. We define the location of the interface $x_I = 5\frac{1}{2}a \approx 9.4$ nm as the distance of the midpoint of these layers to the left electrode. At the left side of the device we take an injection barrier of 0.2 eV, defined as the difference between the Fermi energy of the electrode and the top of the Gaussian DOS of the left organic layer; see Fig. 1.

The Monte Carlo (MC) device simulations proceed in the same way as in Ref. [10]. Like in that work, we take into account both the long-range space-charge effect as well as the short-range effect of Coulomb interactions within a radius R_c. For the results in this work we found $R_c = 8a$ to be sufficient, i.e. an increase of R_c beyond this value does not significantly change the results. In the lateral direction we take 100×100 sites. With this system size and the parameters given above it is sufficient to consider only a single disorder configuration. The error in the currents shown in the plots below is then of the order of or smaller than the symbol sizes. All simulations have been performed at room temperature ($T = 295$ K).

The J–V results obtained by applying the 3D-MC method to our model device are shown by the black squares in Fig. 2, for $\Delta = 0.6$ eV (main figure) and $\Delta = 0$ (inset). For comparison, the current density obtained when neglecting short-range Coulomb interactions is shown by the gray circles. We observe that these interactions strongly affect the current when an internal interface is present, but not in the absence of the interface (the black squares and gray circles in the inset of Fig. 2 coincide). We consider these results as a benchmark. Our goal is to replicate them using a computationally much faster continuum one-dimensional drift–diffusion approach. Although we consider a specific model device, the conclusions that we will reach have a general validity.

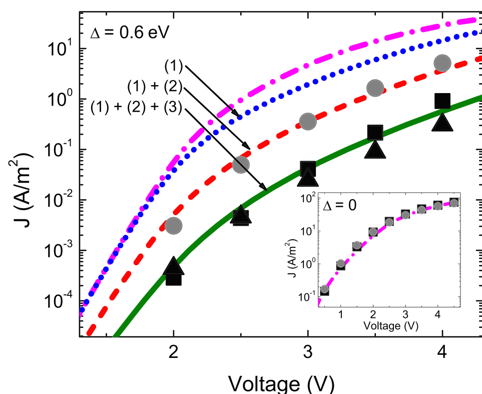

Fig. 2. Current density–voltage characteristics for the device shown in Fig. 1 with $\Delta = 0.6$ eV. Black squares: 3D Monte Carlo (3D-MC) results. Black triangles: 3D-MC results including surface roughness. Gray circles: 3D-MC results without short-range Coulomb interactions. Purple dash-dotted line: 1D drift–diffusion (1D-DD) results assuming thermal equilibrium across the interface. Blue dotted line: 1D-DD results with effect (1) (deviation from equilibrium) included. Red dashed line: 1D-DD results with effects (1) and (2) (non-continuous charge distribution) included. Green solid line: 1D-DD results with effects (1), (2) and (3) (short-range Coulomb interactions) included. Inset: same for $\Delta = 0$, i.e. no internal interface. (For interpretation of the references to colour in this figure legend, the reader is referred to the web version of this article.)

3. One-dimensional drift–diffusion approach

In the continuum 1D-DD approach the carrier density $n(x)$ and electric field $F(x)$ in the device are determined as a function of the distance x from the left electrode by solving the drift–diffusion equation [7]:

$$J = e\mu(x)n(x)F(x) - eD(x)\frac{dn}{dx} = e\mu(x)n(x)\left(F(x) - \frac{1}{e}\frac{dE_F}{dx}\right). \tag{2}$$

Here, e is the elementary charge unit and E_F the Fermi level, which follows from $n(x)$ through the Gauss–Fermi integral. The second equality follows from the generalized Einstein relation [24]. The mobility depends on the position x through its dependence on the local carrier density $n(x)$ and the local electric field $F(x)$. These dependencies, as well as the dependence on temperature T, may be obtained from bulk 3D simulations with a homogeneous carrier density and electric field [8]. The carrier densities at the boundaries of the device are obtained by assuming thermal equilibrium between these boundaries and the electrodes, taking into account the potential change due to the field at these boundaries over a distance a. It is not necessary to take into account the interaction of individual charges with their own images, because of the fairly low injection barrier [9]. The 1D-DD approach is accurate for the basic case of the device with no internal interface ($\Delta = 0$), as may be seen in the inset of Fig. 2 (dash-dotted line).

When modeling the J–V characteristics for the system with an organic–organic interface, a boundary condition should be imposed to connect the carrier density just behind the interface at $x = x_I + a/2$, n_R, to the carrier density just before it at $x = x_I - a/2$, n_L. The dash-dotted line in Fig. 2 shows the J–V curve obtained when thermal equilibrium, true only for $J = 0$, is assumed at the interface, i.e. assuming

$$E_{F,R}(n_R) = E_{F,L}(n_L) + eaF(x_I), \tag{3}$$

where $F(x_I)$ is the electric field at the interface. The dependence of $E_{F,R}(n_R)$ and $E_{F,L}(n_L)$ on the densities n_R and n_L is obtained through the Gauss–Fermi integrals, in which the energy barrier Δ should be accounted for. Fig. 2 shows that this approach gives rise to a too high current density.

There are three separate physical effects that need to be taken into account in order to obtain an appropriate interface boundary condition in the 1D-DD approach:

(1) Deviation from equilibrium: the assumption of thermal equilibrium made in Eq. (3) is not correct; we will show how we can take the effect of the actual non-equilibrium situation into account.
(2) Non-continuous charge distribution: in the 1D-DD model the carrier density profile $n(x)$ is continuous, while in the model device all carriers are located in two-dimensional layers of sites. The effect of this discreteness is especially important in the last layer of sites before the interface, where a large charge density build-up occurs.
(3) Short-range Coulomb interactions: the effective field experienced by a charge attempting to cross the

interface is lower than one would expect based purely on considering the space charge, since the charge does not interact with itself and other charges will be pushed away by the Coulomb repulsion [20].

The results of including these effects are shown in Fig. 2. Including effect (1) leads to the blue dotted line, while including effects (1) and (2) leads to the red dashed line. We note that this result coincides with the 3D-MC simulations without short-range Coulomb interactions (circles). Finally, including all three effects (green solid line) leads to an accurate description of the 3D-MC results in which all effects of Coulomb interactions are included. We note that the 1D-ME method includes effects (1) and (2) in a natural way, since the discreteness of the 3D-MC model is included in this approach. Without any further corrections it provides a fairly good fit (up to about a factor 2) of the 3D-MC results without short-range Coulomb interactions (results not shown).

Below, the methods used to include effects (1)–(3) in the continuum 1D-DD approach are discussed in detail. In the last subsection we will consider a specific case of interface roughness. This leads to a slight change of the J–V characteristics (see the triangles in Fig. 2), but this change is smaller than that due to the above effects.

3.1. Deviation from equilibrium

To obtain a more realistic boundary condition than Eq. (3), we must describe the charge transport over the interface in a manner similar to the bulk by defining a field, a carrier mobility, and a carrier density at the interface. The generalized Einstein relation tells us that a gradient in the Fermi energy has the same effect as an electric field; see Eq. (2). This leads us to the consideration of an effective field

$$F_{\text{eff}} = F(x_{\text{I}}) + (E_{\text{F,L}}(n_{\text{L}}) - E_{\text{F,R}}(n_{\text{R}}))/ea, \tag{4}$$

across the interface. Regarding the mobility and the carrier density we propose taking the geometric average of these quantities at both sides of the interface, leading to the following form of the drift–diffusion equation at the interface:

$$e\sqrt{\mu(n_{\text{L}}, F_{\text{eff}})\mu(n_{\text{R}}, F_{\text{eff}})n_{\text{L}}n_{\text{R}}}\,F_{\text{eff}} = J. \tag{5}$$

We note that, like in the case of Eq. (3), the energy barrier Δ comes into play through the Gauss–Fermi integrals, providing the dependence of the Fermi energies $E_{\text{F,L}}(n_{\text{L}})$ and $E_{\text{F,R}}(n_{\text{R}})$ on n_{L} and n_{R}. We show the results of applying the 1D-DD approach using this boundary condition to our model device in Fig. 2 (dotted line). We see that there is some improvement, but that the agreement is still far from satisfactory.

3.2. Non-continuous carrier distribution

In the top half of Fig. 3 we plot the carrier density distribution in the model device at an applied voltage of 3 V, obtained with 3D-MC modeling (symbols) and the 1D-DD approach with the improved boundary condition discussed above (dotted line). An obvious difference is that in the 1D-DD approach the distribution $n(x)$ is a continuous function of the position x, whereas in the 3D-MC modeling charges can only be present at the discrete positions of the layers of sites of the cubic lattice. This affects the field profile $F(x)$, shown in the bottom half of Fig. 3: in the 1D-DD approach the field increases continuously, while in the 3D-MC modeling it increases discontinuously at the layers of the lattice. This difference is not important in the bulk of the organic layers, because the gradients in $n(x)$ and $F(x)$ are small far from the interface, but it is very significant at the layer just before the interface, where a large build-up of carriers occurs. We note that in a realistic disordered organic semiconductor the sites are not ordered on a lattice, but for a sharp enough interface non-continuum effects at least qualitatively similar to those described here are nonetheless expected to occur.

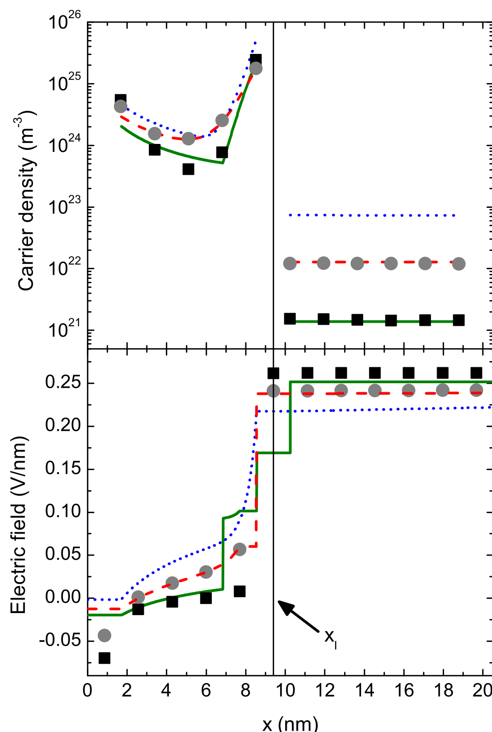

Fig. 3. Charge–carrier density (top) and electric field (bottom) as a function of position in the device shown in Fig. 1, with $\Delta = 0.6$ eV and an applied voltage of 3 V. See Fig. 2 for a description of the curves and symbols. The vertical line indicates the position of the interface x_{I}.

To account for this effect in the 1D-DD approach, we eliminate the unphysical contribution to the space charge of the carrier distribution within a distance $a/2$ of the last layer of sites before the interface. Instead, we add a sheet charge with surface charge density ean_{L} at this layer, which causes a jump in the field equal to $ean_{\text{L}}/\epsilon_0\epsilon_{\text{r}}$. The field profile resulting from the 1D-DD approach with this improvement is shown by the dashed line in the bottom half of Fig. 3. We note that the field stops increasing at a distance $a/2$ before the last layer of sites of the left semiconductor, since we do not consider the contribution to the space

charge there, and then jumps at this layer of sites. This field profile matches the 3D-MC results without short-range Coulomb interactions (circles) quite well, and the same holds for the corresponding density profile. The description of the corresponding J–V characteristics is also excellent; see the dashed line and the circles in Fig. 2.

3.3. Short-range Coulomb interactions

The 3D-MC results displayed in Fig. 2 show that short-range Coulomb interactions play an important role. One might surmise that due to the large carrier density at the interface the charge–carrier mobility is affected by the short-range interactions, and that this should be accounted for in order to obtain an accurate J–V curve. However, we found that, due to the large competition between the drift and diffusion components of the current near the interface, the precise value of the mobility close to the interface is not so relevant for the final current density.

Instead, we find that short-range Coulomb interactions are relevant as a result of the effect of the surface charge just before the interface on the field across the interface. This was first noted by Houili et al. [20]. Up to now we have considered the surface charge at the layer of sites before the interface as laterally homogeneous, which gives an inaccurate description of hops to and from this layer for two reasons: (i) the homogeneous surface charge incorrectly contains a contribution due to the very charge that is hopping (“self-interaction”), (ii) the homogeneous surface charge incorrectly neglects the fact that charges around the one that is hopping will have been pushed away (“Coulomb hole”). As a result, the electric field felt by a carrier hopping over the interface is strongly reduced.

To quantify this reduction of the field, we performed equilibrium MC simulations on a collection of holes in a 2D square lattice, which represents a layer of sites just before the interface. We can then determine the potential difference due to the Coulomb interactions for a charge attempting to hop out of this layer and compare this to the case of a homogeneous surface charge. This procedure accounts for the effects of both the self-interaction and the Coulomb hole. By varying the carrier density n in this layer, the disorder strength σ, and the characteristic energy scale of the Coulomb interactions $U \equiv e^2/4\pi a\epsilon_0\epsilon_r$, we have found that the reduction is well described by multiplying the homogeneous surface charge in this layer by a factor $1 - C$, with C given by

$$C = 0.462 + 0.538\exp(-5.5 n_L/N_t)[1 - \exp(-0.4(U/k_B T)^{0.65})]. \quad (6)$$

Fractions $C/2$ of this surface charge are placed in the two adjacent layers of sites to guarantee charge conservation. The first term in Eq. (6) corrects for the self-interaction and the second for the Coulomb hole. We found that this formula applies for $U/\sigma \gtrsim 2$ (for our model device we have $U/\sigma = 3.1$).

In the 1D-DD approach we apply this procedure only to the last layer of sites before the interface, for which the correction is the most important. This means that the sheet charge with surface charge density ean_L obtained in the previous subsection is multiplied by a factor $1 - C$, while fractions $C/2$ of this sheet charge are placed in the adjacent layers. The resulting field and density profiles (solid lines in Fig. 3) show excellent agreement with the 3D-MC results with all Coulomb interactions included (squares). The same applies to the J–V characteristics; see Fig. 2.

3.4. Interface roughness

With vacuum deposition of organic molecules it is nowadays possible to define layer thicknesses with nanometer precision, i.e. at the scale of the size of a molecule [2]. However, interface roughness at this scale will still occur, while the methods described above apply to a sharp interface. In order to investigate the effects of interface roughness at a scale of one layer of sites we consider a checkered interface, where in the layer before the interface sites corresponding to both organic semiconductors are arranged in a checkerboard pattern. The J–V characteristics resulting from 3D-MC simulations of the modified device are shown by the black triangles in Fig. 2. Although the current is somewhat affected by the interface roughness, it is clear that the three other effects considered above are much more significant. Hence, it is useful to consider the effects discussed in the present work and to apply the developed techniques to obtain an improved modeling by the drift–diffusion approach also to cases for which interface roughness is present.

4. Summary and conclusions

Organic heterojunctions are key ingredients of modern multilayer organic devices and it is essential to develop fast and accurate modeling tools for the charge transport across such junctions. Widely used drift–diffusion approaches to charge transport run into difficulties close to such junctions because the large variations in the charge–carrier density and electric field at the scale of the distance between the localized states involved in the hopping transport prevent a straightforward continuum description. Monte Carlo simulations of the charge transport naturally account for the discreteness in the positions of the localized states and can therefore properly describe the transport across organic heterojunctions. Such simulations are computationally very intensive, but can be used as benchmark for improved drift–diffusion approaches, which can then be used as fast and easy-to-use modeling tools in the industrial development of organic devices.

In this paper the following drift–diffusion approach was developed and shown to match Monte Carlo results, even for a rough interface. (i) Charge transport within the bulk of the organic layers is described as usual by the drift–diffusion equation, Eq. (2). (ii) The boundary condition at the interface, linking the carrier densities n_L and n_R at the left and right side of the barrier, is given by Eq. (5). This boundary condition accounts for the deviation from equilibrium across the interface due the presence of a current. (iii) The unphysical space charge within a distance $a/2$ of the last layer of sites before the barrier, where the carrier density is extremely high, is replaced by a sheet charge at the

location of this layer. This gives rise to a field jump at this layer. (iv) This sheet charge is multiplied by a factor $1-C$, where C is given by Eq. (6), accounting for the self-interaction of the hopping charge and for the Coulomb hole of reduced charge density around this charge, while fractions $C/2$ of this sheet charge are moved to the adjacent layers of sites. The combination of (iii) and (iv) leads to three field jumps: one at the position of the last layer of sites before the barrier, with a size $(1-C)ean_{\mathrm{L}}/\epsilon_0\epsilon_{\mathrm{r}}$, and two at distances $\pm a$ from this layer, with a size $Cean_{\mathrm{L}}/2\epsilon_0\epsilon_{\mathrm{r}}$.

Although the study in this paper has been performed for a specific model device, we expect that the conclusions reached and the approach followed have a general validity for charge transport across organic heterojunctions. We note that a special role is played by the distance a in the approach. In our study it is the lattice constant of the simple cubic lattice we have considered in our Monte Carlo simulations. The finite value of a expresses the positional discreteness of the system of hopping sites. It is this discreteness and not the specific lattice that is the essential complication in continuum drift–diffusion approaches. We therefore expect that our approach can also be applied to realistic organic semiconductors, having a spatially more random distribution of hopping sites. We propose that in that case a should be treated as an effective parameter, which is expected to be of the order of the typical distance between the hopping sites.

Acknowledgements

This work forms part of the research program of the Dutch Polymer Institute (DPI), project No. 680. We thank H. van Eersel for carefully reading the manuscript.

References

[1] Y. Sun, N.C. Giebink, H. Kanno, B. Ma, M.E. Thompson, S.R. Forrest, Management of singlet and triplet excitons for efficient white organic light-emitting devices, Nature 440 (2006) 908.
[2] S. Reineke, F. Lindner, G. Schwartz, N. Seidler, K. Walzer, B. Lüssem, K. Leo, White organic light-emitting diodes with fluorescent tube efficiency, Nature 459 (2009) 234.
[3] C. Tang, S. Van Slyke, Organic electroluminescent diodes, Appl. Phys. Lett. 51 (1987) 913.
[4] S. Van Slyke, C. Chen, C. Tang, Organic electroluminescent devices with improved stability, Appl. Phys. Lett. 69 (1996).
[5] G. He, M. Pfeiffer, K. Leo, M. Hofmann, J. Birnstock, R. Pudzich, J. Salbeck, High-efficiency and low-voltage p-i-n electrophosphorescent organic light-emitting diodes with double-emission layers, Appl. Phys. Lett. 85 (2004) 3911.
[6] C.H. Chang, C.C. Chen, C.C. Wu, S.Y. Chang, J.Y. Hung, Y. Chi, High-color-rendering pure-white phosphorescent organic light-emitting devices employing only two complementary colors, Org. Electron. 11 (2010) 266.
[7] S.L.M. van Mensfoort, R. Coehoorn, Effect of Gaussian disorder on the voltage dependence of the current density in sandwich-type devices based on organic semiconductors, Phys. Rev. B 78 (2008) 085207.
[8] W.F. Pasveer, J. Cottaar, C. Tanase, R. Coehoorn, P.A. Bobbert, P.W.M. Blom, D.M. de Leeuw, M.A.J. Michels, Unified description of charge–carrier mobilities in disordered semiconducting polymers, Phys. Rev. Lett. 94 (2005) 206601.
[9] J.J.M. van der Holst, M.A. Uijttewaal, B. Ramachandhran, R. Coehoorn, P.A. Bobbert, G.A. de Wijs, R.A. de Groot, Modeling and analysis of the three-dimensional current density in sandwich-type single-carrier devices of disordered organic semiconductors, Phys. Rev. B 79 (2009) 085203.
[10] J.J.M. van der Holst, F.W.A. van Oost, R. Coehoorn, P.A. Bobbert, Monte Carlo study of charge transport in organic sandwich-type single-carrier devices: effects of coulomb interactions, Phys. Rev. B 83 (2011) 085206.
[11] E. Knapp, R. Häusermann, H.U. Schwarzenbach, B. Ruhstaller, Numerical simulation of charge transport in disordered organic semiconductor devices, J. Appl. Phys. 108 (2010) 054504.
[12] R. Coehoorn, S.L.M. van Mensfoort, Effects of disorder on the current density and recombination profile in organic light-emitting diodes, Phys. Rev. B 80 (2009) 085302.
[13] M. Schober, M. Anderson, M. Thomschke, J. Widmer, M. Furno, R. Scholz, B. Lüssem, K. Leo, Quantitative description of charge–carrier transport in a white organic light-emitting diode, Phys. Rev. B 84 (2011) 165326.
[14] J. Staudigel, M. Stossel, F. Steuber, J. Simmerer, A quantitative numerical model of multilayer vapor-deposited organic light emitting diodes, J. Appl. Phys. 86 (1999) 3895.
[15] V. Arkhipov, E. Emelianova, H. Bässler, Charge carrier transport and recombination at the interface between disordered organic dielectrics, J. Appl. Phys. 90 (2001) 2352.
[16] E. Tutiš, M. Bussac, B. Masenelli, M. Carrard, L. Zuppiroli, Numerical model for organic light-emitting diodes, J. Appl. Phys. 89 (2001) 430.
[17] T. van Woudenbergh, J. Wildeman, P.W.M. Blom, Charge injection across a polymeric heterojunction, Phys. Rev. B 71 (2005) 205216.
[18] H. Houili, E. Tutis, L. Zuppiroli, Charge transport across organic–organic interfaces in organic light-emitting diodes, Synth. Met. 156 (2006) 1256.
[19] S.W. Tsang, Y. Tao, Z.H. Lu, Temperature dependence of carrier injection across organic heterojunctions, J. Appl. Phys. 109 (2011) 023711.
[20] H. Houili, E. Tutiš, I. Batistić, L. Zuppiroli, Investigation of the charge transport through disordered organic molecular heterojunctions, J. Appl. Phys. 100 (2006) 033702.
[21] A. Miller, E. Abrahams, Impurity conduction at low concentrations, Phys. Rev. 120 (1960) 745.
[22] R.A. Marcus, Electron transfer reactions in chemistry: theory and experiment, Rev. Mod. Phys. 65 (1993) 599.
[23] I. Jurić, I. Batistić, E. Tutiš, Recombination at heterojunctions in disordered organic media: modeling and numerical simulations, Phys. Rev. B 77 (2008) 165304.
[24] Y. Roichman, N. Tessler, Generalized Einstein relation for disordered semiconductors – implications for device performance, Appl. Phys. Lett. 80 (2002) 1948.